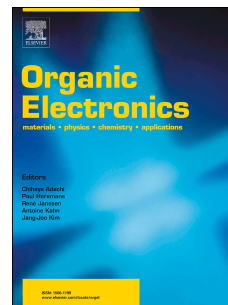# Journal Pre-proof

An insight into the air stability of the benchmark polymer:Fullerene photovoltaic films and devices: A comparative study

Saqib Rafique, Shahino Mah Abdullah, Nafiseh Badiei, James McGettrick, Khue Tian Lai, Nur Adilah Roslan, Harrison Ka Hin Lee, Wing Chung Tsoi, Lijie Li

Please cite this article as: S. Rafique, S.M. Abdullah, N. Badiei, J. McGettrick, K.T. Lai, N.A. Roslan, H.K. Hin Lee, W.C. Tsoi, L. Li, An insight into the air stability of the benchmark polymer:Fullerene photovoltaic films and devices: A comparative study, *Organic Electronics* (2019), doi: https://doi.org/10.1016/j.orgel.2019.105456.

This is a PDF file of an article that has undergone enhancements after acceptance, such as the addition of a cover page and metadata, and formatting for readability, but it is not yet the definitive version of record. This version will undergo additional copyediting, typesetting and review before it is published in its final form, but we are providing this version to give early visibility of the article. Please note that, during the production process, errors may be discovered which could affect the content, and all legal disclaimers that apply to the journal pertain.

An Insight into the Air Stability of the Benchmark Polymer:Fullerene Photovoltaic Films and Devices: A comparative study

Saqib Rafique[1], Shahino Mah Abdullah[2], Nafiseh Badiei[1], James McGettrick[1], Khue Tian Lai[1], Nur Adilah Roslan[2], Harrison Ka Hin Lee[1], Wing Chung Tsoi[1] and Lijie Li[1*]

[1]*Multidisciplinary Nanotechnology Centre and SPECIFIC, College of Engineering, Swansea University, Swansea SA1 8EN, United Kingdom*

[2]*Low Dimensional Materials Research Centre, Department of Physics, Faculty of Science, University of Malaya, 50603 Kuala Lumpur, Malaysia.*

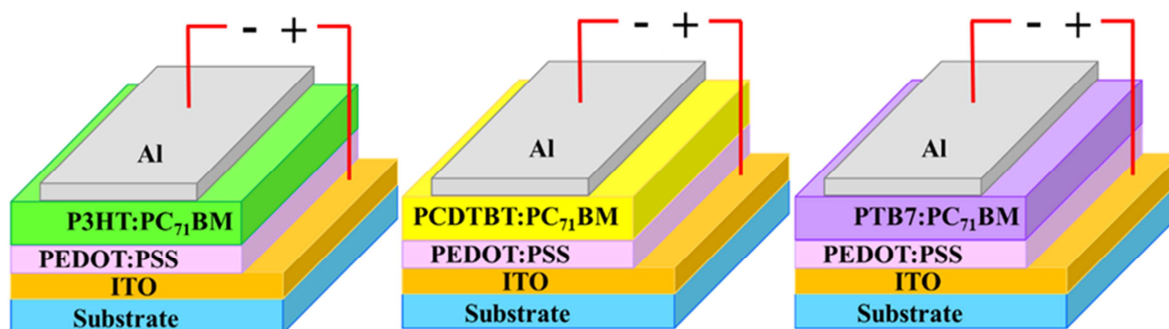*Corresponding author: l.li@swansea.ac.uk

An Insight into the Air Stability of the Benchmark Polymer:Fullerene Photovoltaic Films and Devices: A comparative study

Saqib Rafique[1], Shahino Mah Abdullah[2], Nafiseh Badiei[1], James McGettrick[1], Khue Tian Lai[1], Nur Adilah Roslan[2], Harrison Ka Hin Lee[1], Wing Chung Tsoi[1] and Lijie Li[1*]

[1]*Multidisciplinary Nanotechnology Centre and SPECIFIC, College of Engineering, Swansea University, Swansea SA1 8EN, United Kingdom*

[2]*Low Dimensional Materials Research Centre, Department of Physics, Faculty of Science, University of Malaya, 50603 Kuala Lumpur, Malaysia.*

*Corresponding author: l.li@swansea.ac.uk

ABSTRACT

In this study, a comparative analysis of the instabilities and degradation routes of organic solar cell (OSCs) employing the three benchmarked donor polymers namely poly(3-hexylthiophene) (P3HT), poly[N-900- hepta-decanyl-2,7-carbazole-alt-5,5-(40,70-di-2-thienyl-20,10,30-benzothiadiazole)] (PCDTBT) and Poly[[4,8-bis[(2-ethylhexyl)oxy]benzo[1,2- b:4,5-b']dithiophene-2,6-diyl][3-fluoro-2-[(2 ethylhexyl)carbonyl] thieno[3,4-b]thiophenediyl]] (PTB7) along with [6,6]-phenylC$_{71}$ butyric acid methyl-ester (PC$_{71}$BM) acceptor have been conducted using the extracted photovoltaic parameters in conjunction with the X-ray photoelectron spectroscopy (XPS), optical and morphological analysis. During the 14 days air stability test, the power conversion efficiency (PCE) decreased by 78.85%, 65.83% and 83.36 % for P3HT:PC$_{71}$BM, PCDTBT:PC$_{71}$BM and PTB7:PC$_{71}$BM based devices, respectively. However, the degradation study of the bulk heterojunction (BHJ) films was prolonged to 28 days in order to further elucidate the degradation factors affecting the device performance. XPS, optical and morphological studies enabled detailed information on the device degradation mechanisms and confirmed the oxidation of photoactive layer after ageing, morphological deterioration and fall in absorbance, particularly, the PTB7:PC$_{71}$BM blend that showed the rapid degradation among all three. The results obtained in the current studies advance the understanding of the stability/degradation mechanisms pertaining to the three most commonly used BHJ materials and hence, will help to improve the OSCs for longer lifetime.

1. INTRODUCTION

Recent years have witnessed the remarkable progress in the organic semiconductors and received tremendous attention from the scientific community. These materials possess several advantages owing to their facile synthesis methods, low cost, environmental friendliness, excellent transparency, flexibility, and tunable optoelectronics properties [1-3]. In the organic photovoltaic field, the emergence of new materials has pushed the power conversion efficiencies (PCEs) beyond the 10% [4-9]. However, prolonged lifetime is equally essential along with the high PCEs for their successful commercialisation, but very less is known about the operational and environmental stability of these solar cell modules. Nevertheless, the lifetime is still needed to be improved before large scale production can become significant. Therefore, understanding the degradation mechanisms that hinder the operational stability of organic solar cells (OSCs) under various environmental factors is a prerequisite. In this context, it is the prime concern of research community to address the instability of the polymer/fullerene absorption layer caused by the intrinsic and extrinsic degradation factors.

The most studied OSCs employ the regioregular poly(3-hexylthiophene) (P3HT) as donor material combined with the fullerene based acceptors such as [6,6]-phenylC_{71} butyric acid methyl-ester ($PC_{71}BM$) to form a morphologically stable bulk heterojunction (BHJ) photoactive layer [10]. P3HT is typically a crystalline photovoltaic polymer that is deposited by facile solution processing followed by the evaporation of metallic cathode (back electrode), which constructs a so-called normal architecture device. It facilitates the flow of electrons from the transparent electrode to the back electrode (**Figure 1b**) to yield an efficiency of 3 to 5% [11]. However, Sarah *et al.*[12] demonstrated an efficiency of 6.4% that is the highest reported for fullerene-free P3HT devices. Over the years, new donor polymers with high efficiencies have

emerged. For example, amorphous copolymer based on poly(2,7-carbazole) derivatives of poly[N-900- hepta-decanyl-2,7-carbazole-alt-5,5-(40,70-di-2-thienyl-20,10,30-benzothiadiazole)] (PCDTBT) has demonstrated high efficiencies and photo-current generation owing to its faster charge carrier generation capability and different recombination dynamics as compared to P3HT [13-15]. Recently, the low band-gap polymer, Poly[[4,8-bis[(2-ethylhexyl)oxy]benzo[1,2- b:4,5-b']dithiophene-2,6-diyl][3-fluoro-2-[(2 ethylhexyl)carbonyl] thieno[3,4-b]thiophenediyl]] (PTB7) demonstrated very promising results with the blend PTB7:PC$_{71}$BM as photoactive layer compared with P3HT and PCDTBT [16, 17]. However, a number of studies showed that PTB7 is a relatively unstable material [18, 19].

This work focuses on the device lifetime of three OSC variants employing P3HT, PCDTBT and PTB7 donor polymers along with the PC$_{71}$BM acceptor as photoactive layer. It is important to understand the mechanism of device degradation during its operation in order to get optimized device having longer lifetime. Materials degrade due to deterioration in their chemical, optical, morphological and electrical properties [10]. Photovoltaic devices are very sensitive to even small degree of degradation. It is thus critical for the successful device operation to remove or at least mitigate degradation in order to improve the stability. Particularly, polymer/fullerene BHJ films can be easily deteriorated due to various chemical and physical degradation pathways. In OSCs, each of the photoactive materials has distinguished morphological, chemical, optical and photovoltaic properties, therefore, they predominantly respond differently to the atmospheric degradation and the physical and chemical degradation may occur at different rates for each of the P3HT:PC$_{71}$BM, PCDTBT:PC$_{71}$BM and PTB7:PC$_{71}$BM BHJ layers.

In this study, therefore, it is aimed to analyze and compare the air stability behavior of three different and most commonly used bench marked BHJ donor-acceptor materials, both for films and devices. The work has two-fold significance. Firstly, it reports the air stability of polymer: fullerene photovoltaic films/devices, which has been rarely reported earlier. Hence, we believe that it is a substantial study which will definitely help to improve the OSCs for longer lifetime. Secondly, it gives a comprehensive and comparative analysis of the three most commonly used donor-acceptor materials in one paper and it makes a lot easier for a reader to determine and compare the merits and demerits of each of the material. Photovoltaic performance has been measured, and morphological, optical and chemical changes have been evaluated to elucidate the degradation patterns and hence, the failure mechanisms in normal architecture solar cells. Evaluation of device performance and degradation mechanisms have been carried out using current density-voltage (*J-V*) measurements, UV-visible absorbance study, X-ray photoelectron spectroscopy (XPS), atomic force and field emission-scanning electron microscopy (AFM and FESEM) analysis. All these methods were used to quantitatively and qualitatively compare the performance of OSCs in terms of their air stability and degradation.

2. EXPERIMENTAL SECTION

2.1 Materials

Pre-patterned indium tin oxide (ITO) glass substrates (sheet resistance of ~15 $\Omega/\square$) were purchased from Ossila Ltd., UK. The photoactive materials namely, P3HT, PCDTBT, PTB7 and PC$_{71}$BM were purchased from Lumtec Corp. Taiwan. PEDOT:PSS was obtained from H.C. Stark.

2.2 Fabrication of P3HT:PC$_{71}$BM, PCDTBT:PC$_{71}$BM and PTB7:PC$_{71}$BM Based Normal Architecture Solar Cells

Normal architecture solar cells employing P3HT:PC$_{71}$BM, PCDTBT:PC$_{71}$BM and PTB7:PC$_{71}$BM as photoactive blend layers were fabricated on prepatterned ITO coated glass substrates. For the fabrication of solar cells, ITO substrates were first cleaned with detergent, subsequently sonicated in acetone and isopropanol for 15 min followed by rinse in deionized (DI) water and nitrogen blow dry. The samples were immediately treated with oxygen plasma for 2.5 min. PEDOT:PSS was (first filtered with 0.45μm PTFE filters (Whatman, Germany)) deposited by spin coating on top of ITO at 4000 rpm for 40 s and annealed at 120 °C for 30 min in the air. The samples were then transferred to the glovebox to deposit the photoactive layer.

The first polymer-fullerene blend solution was prepared by dissolving P3HT and PC$_{71}$BM in a 1.0:0.6 ratio (25:15 mg in mL of chlorobenzene) in 1 mL of chlorobenzene. The solution was stirred for ∼24 h at 60 °C prior to deposition. The blend was spun coated at 900 rpm for 45 s to yield a 200 nm thick layer followed by annealing at 110 °C for 10 min on a hotplate. PCDTBT:PC$_{71}$BM was prepared by dissolving in chlorobenzene and mixing by vigorous stirring at the ratio of 1:4 (6mg:24mg in 1mL chlorobenzene). The blend was spun cast at an optimized speed of 2000 rpm for 40 s to deposit an ∼70 nm thick layer. The PTB7:PC$_{71}$BM blend with 1:1.5 w/w ratio (10mg:15mg in 1mL chlorobenzene) was prepared in chlorobenzene. The homogenized solution was obtained by stirring for ∼24 h at 30 °C. The photoactive layer was obtained by spin casting in a glovebox yielding a thickness of 100 nm at 1200 rpm for 60 s. Later, the ITO/PEDOT:PSS/photoactive layer structure was transferred to the thermal evaporator to deposit 100 nm thick aluminum (Al) cathode in vacuum ($< 10^{-6}$ Torr).

6

2.3 Photovoltaic Characterization

The *J-V* characteristics were measured using a Keithley 236 (Keithley Co.) source measuring unit. The solar cells were illuminated with a calibrated Newport solar simulator equipped with a xenon lamp, providing an AM 1.5 G spectrum with an irradiation intensity of 100 mW/cm^2 as measured by the Newport power meter 1918-R. The long-term ageing was performed in the ambient air. The air stability test included an oxygen atmosphere at room temperature for a total period of 14 days. Photovoltaic characterizations were repeated after as-cast, 7 and 14 days to record the decay in the photovoltaic parameters. For each variant, six devices were fabricated to give an average value [20]. Hence, a total of eighteen devices were characterized to ensure the reproducibility and reliability of the results.

2.4 Characterization of Degradation Mechanism

ITO/PEDOT:PSS/BHJ photoactive layer films were replicated following same fabrication procedure and characterized on the surface of photoactive layer for composition, morphology, optical properties and chemical changes to qualitatively and quantitatively evaluate the degradation as a function of 28 days of storage in ambient air. An atomic force microscope (AFM, JPK Nano Wizard II) was utilized to obtain the surface morphology images of the samples. AFM images (512 scan lines and 512 pixels per scan line) were acquired using the tapping mode. The images were then subjected to a 3rd order flattening procedure using the Bruker NanoScope Analysis V1.40 software to remove the non-linear background artifacts introduced by the piezo scanner. Following the flattening procedure, the surface roughness was quantified over 5 µm x 5 µm scan size images. Scanning electron Microscope, SEM (Hitachi 4800 S, Japan) was used to image the polymers. The change in the absorbance of the photoactive layer as a function of ageing in ambient air were recorded over the range of 300 to 800 nm using

a double- beam UV/Vis/NIR Perkin-Elmer Lambda 365 spectrophotometer. XPS measurements were performed using a Kratos Axis Supra (Kratos Analytical) X-ray Photoelectron Spectrometer equipped with a monochromated Al- Kα source. Peak fittings of the deconvoluted data were determined using the Kratos sensitivity factor library on Casa XPS (2.3.17dev6.4k) software.

3. RESULTS

Figure 1 (a-d) displays the device architecture employing different BHJ layers, molecular structure of the constituent materials, their energy level diagram and the *J-V* characteristics of the OSC variants, respectively. The ageing of the devices with the following general configuration of ITO/PEDOT:PSS/P3HT:PC$_{71}$BM/Al, ITO/PEDOT:PSS/PCDTBT:PC$_{71}$BM/Al, ITO/PEDOT:PSS/PTB7:PC$_{71}$BM/Al and their replicated films were conducted in the air to check the air stability in the oxygen (O$_2$) atmosphere and at room temperature (25°C). Three variants of OSCs were tested for stability for 14 days. However, the degradation study of the BHJ layers was prolonged to 28 days in order to elucidate the degradation factors affecting the device performance. It has been known for a long time that atmospheric induced penetration of oxygen and water into the device lead to some of the most pronounced degradation mechanisms for OSCs. In this work, we seek a more detailed and comparative understanding of this phenomenon by using the three most commonly used BHJ donor-acceptor materials. Although, degradation is a range of complex mechanisms such as; degradation of photoactive layer, degradation of interfaces, electrode diffusion and reaction with the organic materials, morphological deterioration and formation of cracks and bubbles *etc.*, however, the focus of the current study will be on identifying the degradation factors pertaining

to the photoactive materials, and therefore, the degradation results related to the photoactive layer will be discussed in this paper.
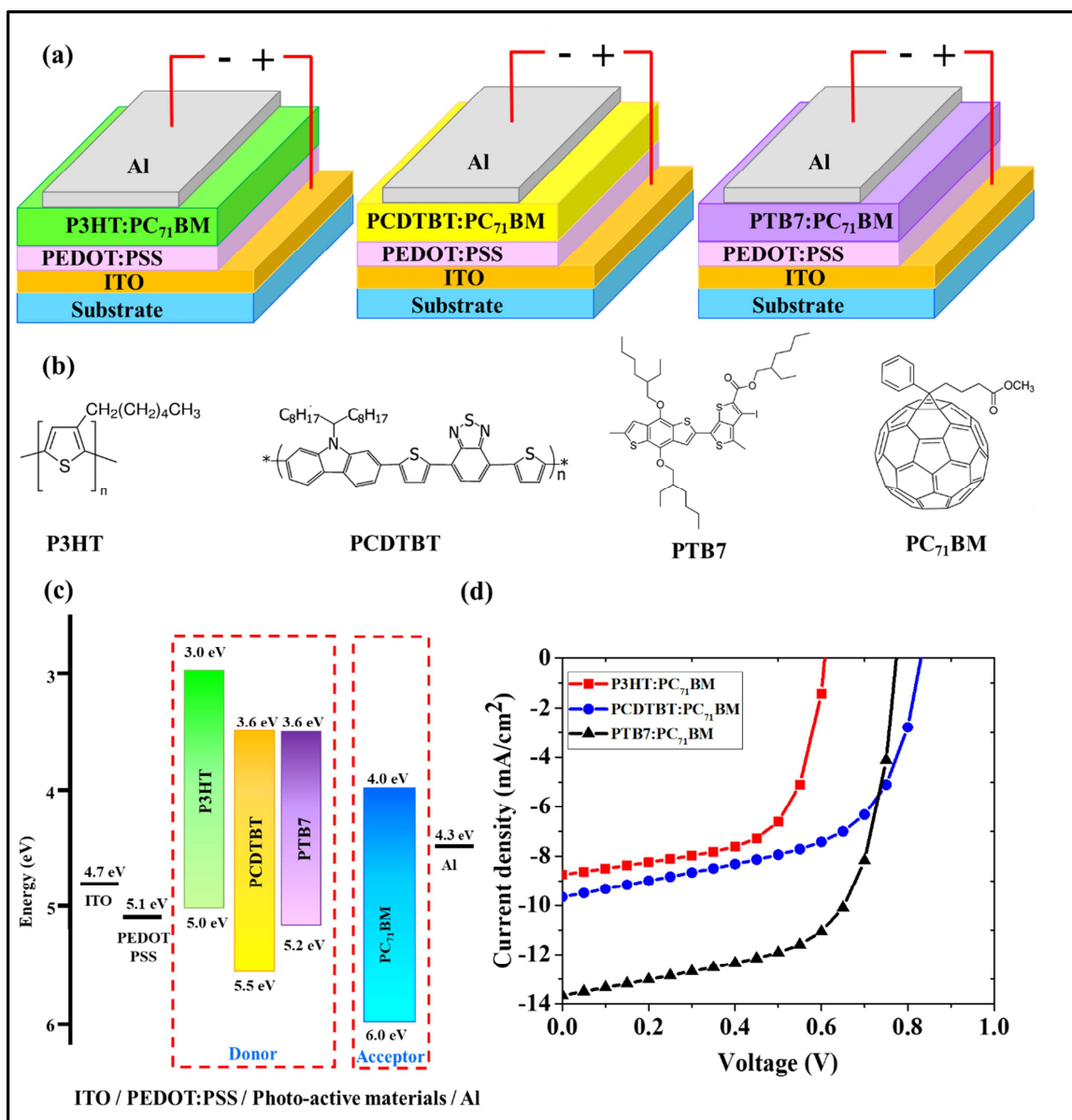

Figure 1: **(a)** Schematic of the device architecture employed with P3HT:PC$_{71}$BM, PCDTBT:PC$_{71}$BM and PTB7:PC$_{71}$BM BHJ photoactive layers characterized as a function of storage in ambient atmosphere to test the ambient stability. **(b, c)** Molecular structures and energy levels of the photovoltaic materials (P3HT, PCDTBT, PTB7 and PC$_{71}$BM). **(d)** *J-V*

9

curves of the traditional structured OSCs based on P3HT:PC$_{71}$BM, PCDTBT:PC$_{71}$BM and a PTB7:PC$_{71}$BM BHJ photoactive layer prior to degradation.

3.1 Time Evolution of Photovoltaic Performance

Figure 2 shows the *J-V* characteristics of the **(a)** P3HT:PC$_{71}$BM, **(b)** PCDTBT:PC$_{71}$BM and **(c)** PTB7:PC$_{71}$BM based solar cells. The most optimised polymer/fullerence ratios were chosen based on the best performing devices reported in the literature. The average values of the the key performance data; short-circuit current density (J$_{sc}$), fill factor (FF), open circuit voltage (V$_{oc}$) and PCE were obtained for as-cast, 7 days and 14 days of aging and are summarised in **Table 1**. Whereas, the error bars in the **Figures S1-S3** denote standard deviation. It is noteworthy that some of the device performance values may be below the best reported values for that device structrue, however, the sole purpose of this work is to carry out a comparative study in order to understand the degradation of the most commonly used BHJ materials rather to produce the so-called best-performing "hero" devices. Thus, the performance parameters are still comparable with the literature and can be used to obtain a general picture of the degradation behavior. The investigated solar cells showed an average PCE of 3.31% (V$_{oc}$= 0.61 V, J$_{sc}$= 8.74 mA/cm^2 and FF= 0.62) for P3HT that has reduced to 0.70% in 14 days (V$_{oc}$= 0.55 V, J$_{sc}$= 5.78 mA/cm^2 and FF= 0.22). The device employing P3HT donor polymer exhibited 78.85% efficiency loss mainly due to drastic decrease in the FF (64.51% loss) followed by 33.87% loss in the J$_{sc}$. However, the V$_{oc}$ (9.83%) remained relatively stable as compared to other performance indicators. The device with PCDTBT donor polymer showed a PCE drop of 65.83% (PCE reduced from 5.18% to 1.77%) in 14 days mainly due to a significant drop in FF (52.46% loss) followed by 22.62% loss in the V$_{oc}$. However, the J$_{sc}$ showed relatively stable values and exhibited only 7.13% loss. Lastly, the device with PTB7 donor polymer showed a PCE of 6.61%

that had reduced to 1.10% in 14 days, exhibiting the highest drop in the PCEs (83.36%) among the three donor polymers under study. The reduction in the PCE is attributed to a drastic decrease in the FF (61.29% loss) and J_{sc} (45.87%) followed by 20.51% loss in the V_{oc}. More details from the $J-V$ curve analysis for all three variants are presented in **Table 1.**

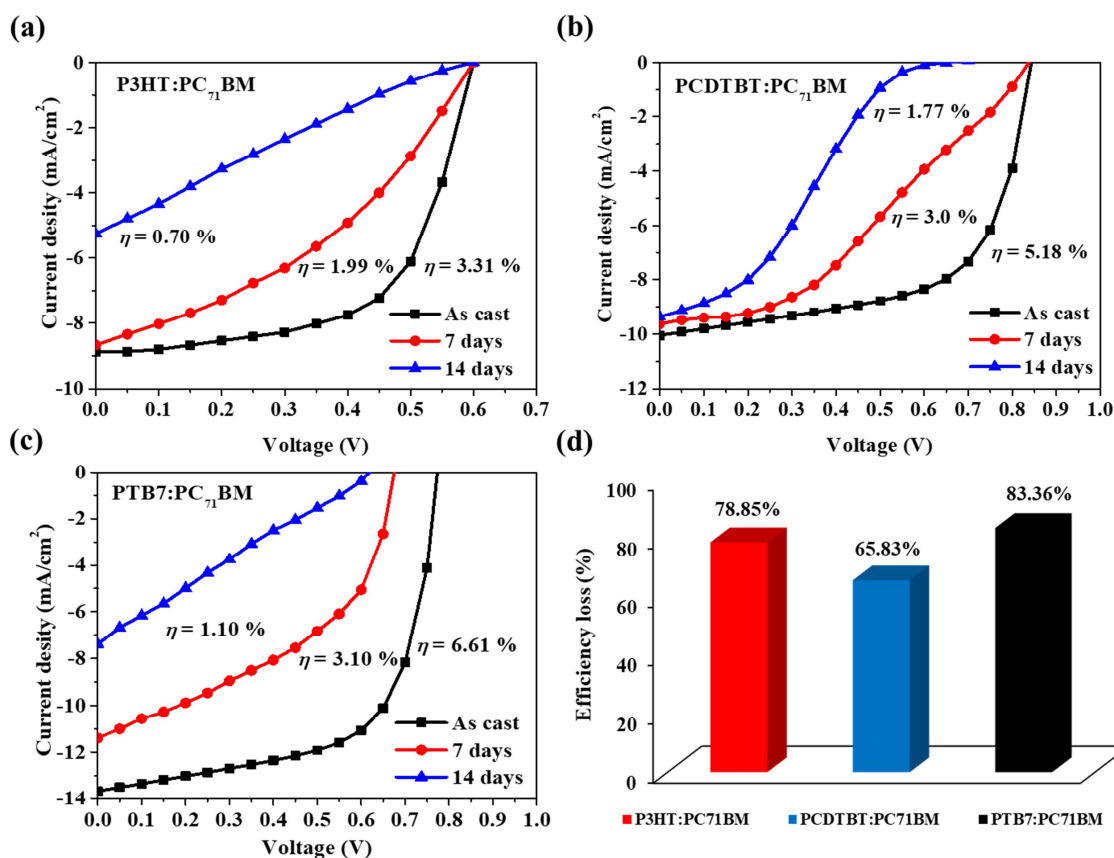**Figure 2:** J-V characteristics of the OSC devices with **(a)** P3HT:PC$_{71}$BM, **(b)** PCDTBT:PC$_{71}$BM and **(c)** PTB7:PC$_{71}$BM BHJ photoactive layers as a function of storage in ambient air for up to 14 days. **(d)** Efficiency loss (%) in 14 days.

Table 1: Key performance data of solar cells comprising P3HT:PC$_{71}$BM, PCDTBT:PC$_{71}$BM and PTB7:PC$_{71}$BM BHJ photoactive layers in terms of percentage loss (along with real parameters) as a function of ageing in air. Data was averaged from eighteen devices, whereas, the error bars in the **Figure S1-S3** represent the standard deviation.

BHJ layer	Storage time	J_{sc} [mA/cm^2]	*Jsc* decay [%]	V_{oc} [V]	V_{oc} decay [%]	FF [%]	FF decay [%]	PCE [%]	PCE decay[%]
P3HT:PC$_{71}$BM	As-cast	8.74		0.61		0.62		3.31	
	7 days	8.67	33.87	0.56	9.83	0.41	64.51	1.99	78.85
	14 days	5.78		0.55		0.22		0.70	
PCDTB:PC$_{71}$BM	As-cast	10.1		0.84		0.61		5.18	
	7 days	9.63	7.13	0.82	22.62	0.38	52.46	3.00	65.83
	14 days	9.38		0.65		0.29		1.77	
PTB7:PC$_{71}$BM	As-cast	13.67		0.78		0.62		6.61	
	7 days	11.39	45.87	0.68	20.51	0.40	61.29	3.10	83.36
	14 days	7.4		0.62		0.24		1.10	

3.2 Investigating the Degradation Mechanisms of Polymer/Fullerene BHJ Blends.

To monior the degradation of the BHJ photoactive materials, films were replicated on ITO following the *ITO/PEDOT:PSS/BHJ* layer configuration and aged in ambient air. The photovoltaic performanc of the corresponding devices has already been discussed above. While the degradation study was prolonged to 28 days to further investigate the morphological, optical and chemcial changes in the absorption layer. Hence, it will provide a much deeper understanding of degradation factors affecting the device performance, particularly, the BHJ layer. We conducted XPS, SEM, AFM and UV-visible studies on the aged films and data are analyzed for as-cast and up to 28 days.

3.2.1 Chracterisation of Morphological and Optical Degradation

The optical properties of the photoactive layer play an important role in OSCs. In order to investigate the impact of the air induced degradation on the films, we first analyzed the absorbance of glass/ITO/PEDOT:PSS/BHJ photoactive blends up to 28 days with equal interval of 7 days. **Figure 3** shows the absorbance spectra of **(a)** P3HT:PC$_{71}$BM, **(b)** PCDTBT:PC$_{71}$BM and **(c)** PTB7:PC$_{71}$BM recorded between 300 and 800 nm. The results clearly indicate the very good stability in the absorbance of P3HT:PC$_{71}$BM and PCDTBT:PC$_{71}$BM films with insignificant change (deviation of $\pm 1\%$) in the corresponding spectra over the period of 28 days. However, the PTB7:PC$_{71}$BM showed more pronounced reduction and showed up to 8% (**Figure 3d**) reduction in the absorbance with maximum decay for the peak at 564 nm, indicating that PTB7 is more prone to atmospheric induced degradation upon its exposure to air.
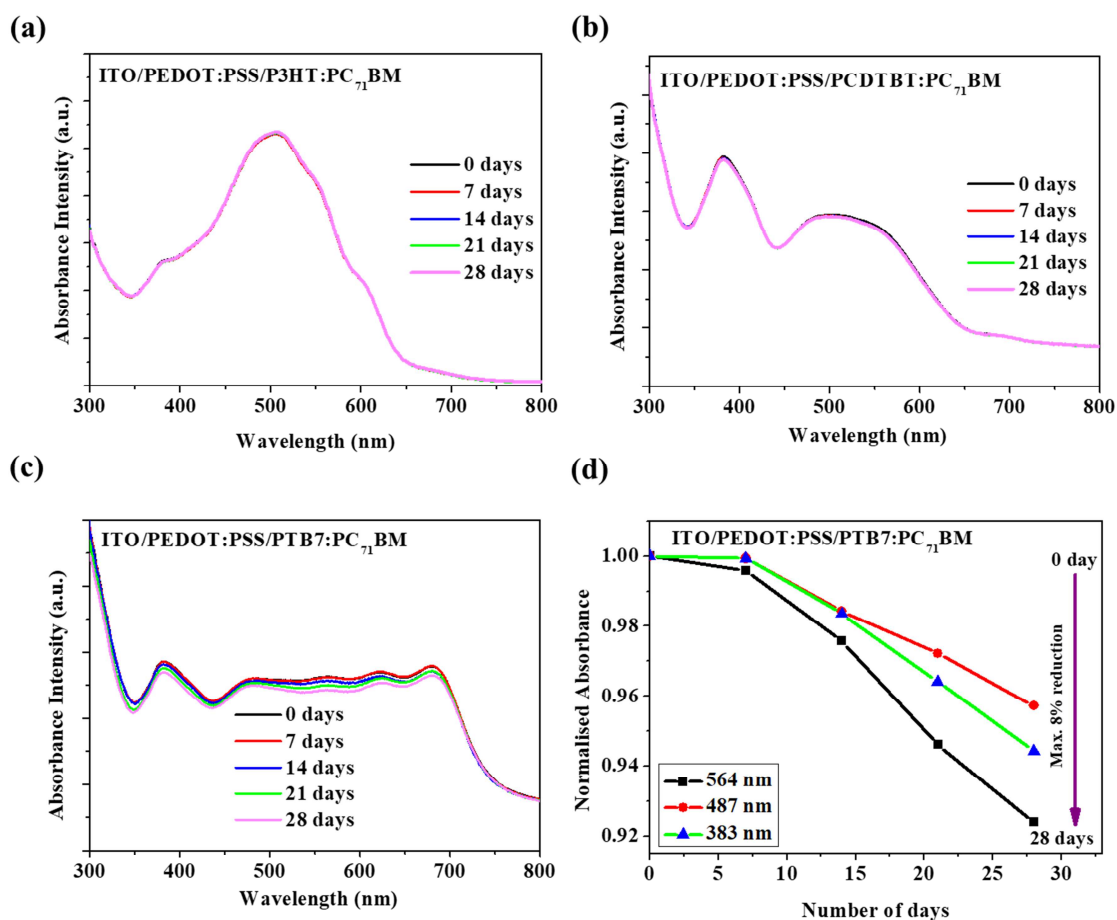
Figure 3: Decay in the UV-vis absorbance spectra of *glass/ITO/PEDOT:PSS/photoactive material* as a function of 28 days storage in ambient air based on **(a)** P3HT:PC$_{71}$BM, **(b)** PCDTBT:PC$_{71}$BM and **(c)** PTB7:PC$_{71}$BM BHJ photoactive layers. **(d)** Decay in the absorbance of ITO/PEDOT:PSS/PTB7:PC$_{71}$BM analyzed for the peaks at 383, 487 and 564 nm up to 28 days of storage in ambient air.

2-dimensional (2D) and 3D AFM topography images of the BHJ layer were recorded to probe the morphological variation before and after the degradation. While the SEM micrographs of the same have been presented in the **Figure S4** of the "Supplementary Information". It is

noteworthy that the morphology of the donors and acceptors (BHJ blend) significantly influences the dissociation and transportation of charge carriers [21]. Also, it induces the charge recombination. **Figure 4** shows the evolution of the surface morphology of P3HT:$PC_{71}BM$, PCDTBT:$PC_{71}BM$ and PTB7:$PC_{71}BM$ BHJ surfaces in the tapping AFM mode before and after 28 days of storage in ambient air. The P3HT:$PC_{71}BM$ (**Figure 4a, b**) and PCDTBT:$PC_{71}BM$ (**Figure 4c, d**) films are very uniform and smooth displaying a root-mean-square roughness (RMS) of 1.92 and 1.05 nm for the as-cast films that possessed no significant change in the RMS values after 28 days of storage in ambient air. Interestingly, the RMS value decreased to 1.34 nm (although the same is insignificant) for the P3HT:$PC_{71}BM$ which indicates the slight smoothing and planarization of the surface over the 28 days of storage in ambient air. However, it increased to 1.77 nm for the PCDTBT:$PC_{71}BM$ BHJ film. **Figure 4e and f** display the surface morphology of the PTB7:$PC_{71}BM$ BHJ layer before and after the ageing with corresponding RMS of 3.29 and 5.81 nm, respectively, indicating that the air induced degradation has significantly influenced the PTB7:$PC_{71}BM$ BHJ layer and RMS surface roughness has increased to almost double of the as-cast film. In the aged sample (**Figure 4f**) protruding nano-spheres of slightly varying diameters are observed. These similar sized features of aggregates have also been observed in the SEM micrographs, and also in good agreement with the reported data [22-25]. The observed increase of roughness as a result of deterioration of BHJ layer, particularly in the case of PTB7:$PC_{71}BM$, is also complemented by the corresponding decrease in the device performance as well as the decrease in the optical absorbance and the chemical changes analyzed by the XPS.
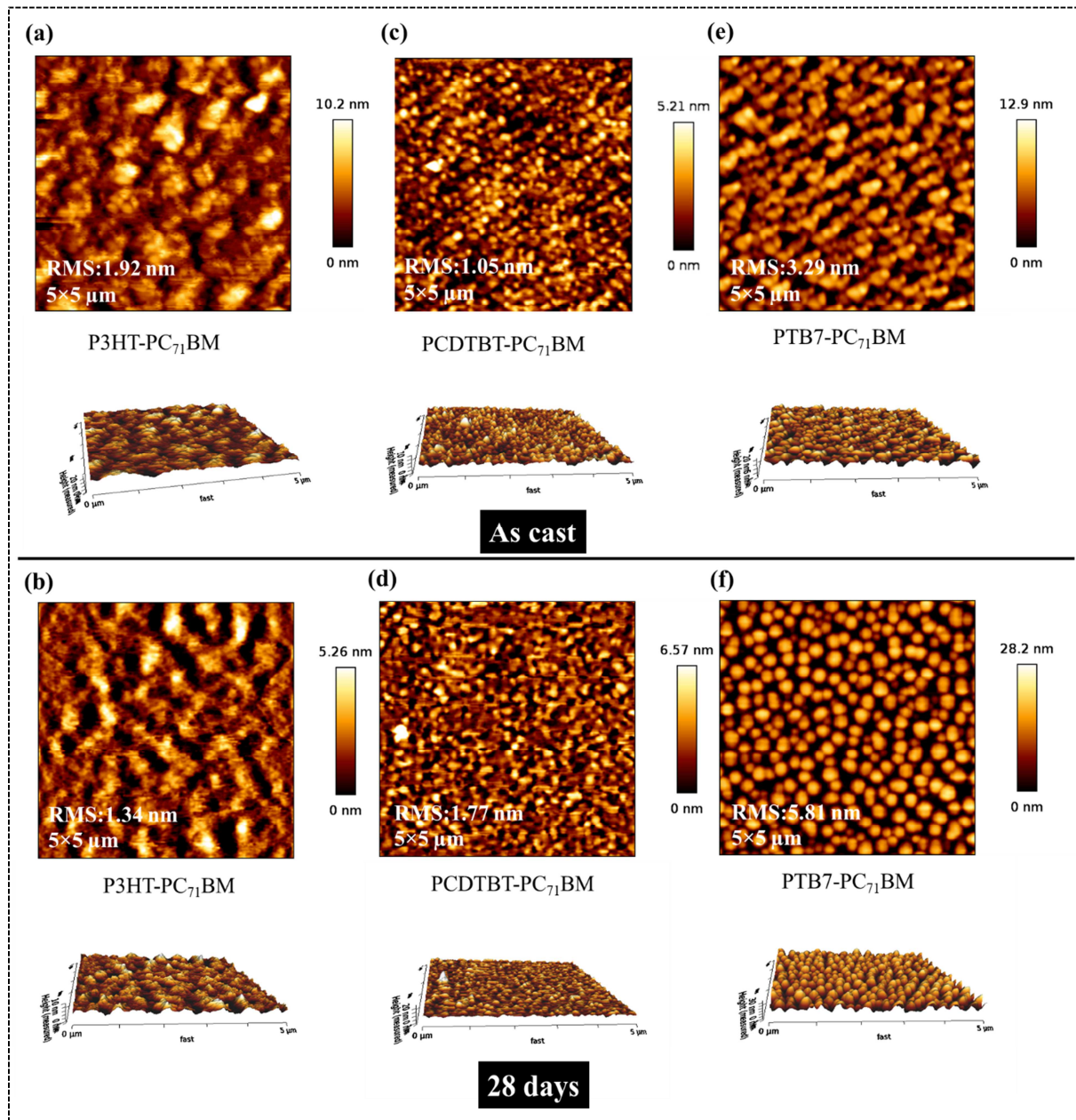
15

Figure 4: 2D and 3D topography AFM images (5 µm× 5 µm) of as-cast and after 28 days of storage in ambient air for **(a, b)** P3HT:PC$_{71}$BM, **(c, d)** PCDTBT:PC$_{71}$BM and **(e, f)** PTB7:PC$_{71}$BM films, deposited on top of ITO/PEDOT:PSS.

SEM micrographs were obtained in order to acquire complementary information about surface changes as the function of storage time in ambient air. The SEM images of the BHJ surface for all three variants obtained for as-cast and after 28 days of storage in ambient air are presented in the **Figure S4**. The images reveal smooth polymer surface of the as-cast films, with morphology features very similar to that observed in the AFM images. Rarely, some clusters of the organic materials have been found on the degraded samples of P3HT:PC_{71}BM and PCDTBT:PC_{71}BM (*e.g.* marked in **Figure S4 b and d**). However, as discussed in the AFM results too, the PTB7:PC_{71}BM films show a granular surface, whereas, a slight increase in the grain size can be seen in PTB7:PC_{71}BM BHJ after ageing. This change in roughness and grain size will affect the absorbance as well as the photovoltaic properties of the corresponding device as evident in our results too.

3.2.2 Surface Analysis for Chemcial Changes With Ageing Using XPS

In order to elucidate the mechanisms accounting for the degradation of OSCs and specifically the BHJ layer, XPS was employed to determine the chemical states and the relative changes in the surface composition which occurred during ageing. XPS is very useful tool to monitor the chemical changes in the outer 5-10 nm of the surface during ageing in an ambient atmosphere with some specificity. Therefore, the chemical changes and hence the degradation mechanisms can be deduced from the distinguished spectra of the corresponding elements. Two types of information were extracted: **(i)** the high-resolution spectra that particularly contains (among others) the chemical states information and **(ii)** the elemental composition. **Table 2** shows the atomic concentration for all three variants of BHJ films for as cast and aged samples. As expected, the oxygen content has increased with ageing time for all three BHJ variants and reached to almost double of the initial values suggesting that oxidation of materials has occurred

during the ageing [10, 26]. It is noteworthy that oxygen (O1s) concentration (the absolute value) substantially increased to 10.5 % in the case of PTB7:PC$_{71}$BM which indicates the oxygen induced degradation of this material at accelerated rates as compared to the BHJ layers comprising of P3HT and PCDTBT based donor polymers. For P3HT:PC$_{71}$BM and PCDTBT:PC$_{71}$BM samples, the O1s content has increased from 0.5 to 3.61% and 2.3 to 5.63%, respectively. The effect of oxidation has been observed in the corresponding decay of photovoltaic and other properties too, in good agreement with our findings. Almost 4 ± 0.5 % reduction in the carbon (C1s) content has been observed in all three BHJ films. Whereas, the sulfur (S2p) has slightly reduced in the case of P3HT:PC$_{71}$BM (6.85 to 5.26%) and PTB7:PC$_{71}$BM (4.42 to 4.00%) but PCDTBT:PC$_{71}$BM exhibited almost negligible change. Similarly, the change in concentration of nitrogen (N1s) of PCDTBT:PC$_{71}$BM and fullerene (F1s) of PTB7:PC$_{71}$BM is also insignificant over the period of 28 days.

Table 2: The relative atomic concentration in P3HT:PC$_{71}$BM, PCDTBT:PC$_{71}$BM and PTB7:PC$_{71}$BM BHJ films before (as-cast) and after 28 days of storage in ambient air (aged).

Element		Atom % concentration		
		P3HT:PC$_{71}$BM	PCDTBT:PC$_{71}$BM	PTB7:PC$_{71}$BM
C1s	As-cast	92.65	90.2	86.17
	Aged	88.96	86.16	82
O1s	As-cast	0.5	2.3	6.1
	Aged	3.61	5.63	10.5
S2p	As-cast	6.85	1.95	4.42
	Aged	5.26	2	4
F1s	As-cast	-	-	3.29
	Aged	-	-	3.45
N1s	As-cast	-	4.64	-
	Aged	-	4.7	-

Figure 5 (a-d) displays the C1s high-resolution XPS spectra for **(a, b)** P3HT:PC$_{71}$BM and **(c, d)** PCDTBT:PC$_{71}$BM. The XPS spectra show minor changes other than in the C-C and C-O bonds, for which the peaks have become slightly more prominent after 28 days of storage in ambient air, owing to the oxidation of BHJ material [27]. The C1s spectra for both blends show the sp^2 and sp^3 carbon components at 284.3 eV and 284.8 eV, corresponding to the C=C and C-C bonds (non-oxygenated bonds), respectively. These assignments are in good agreement with previous works [28, 29]. Also, there are peaks at 285.9 and 286.9 eV, which are attributed to the C-O [30-32] and C=O [33, 34] bonds, respectively, and represent the oxygen-containing components (carbon atoms bonded with oxygen). As discussed earlier, the C-O and C=O peaks appeared to be slightly more prominent and sharper, which indicates the excess of oxygen compared to the as-cast films, as evident in **Table 2**. However, in the case of PTB7:PC$_{71}$BM BHJ sample, even for the as-cast sample the C1s spectra appeared as typical of an oxygen-containing polymer with relatively prominent peaks for C-O and C=O bonds. After the degradation, the spectra in **Figure 5f** clearly indicate the considerable degree of oxidation and the peaks representing the carbon singly or doubly bonded to oxygen (oxygen-bonded species) are considerably increased [19, 35]. These oxidized species can potentially cause the degradation of the BHJ materials, leading to an inability of the polymer:fullerene blend to transfer the charge [29, 36, 37], while the peak intensities for both the sp^2 and sp^3 carbon components (C=C and C-C) have been significantly reduced.
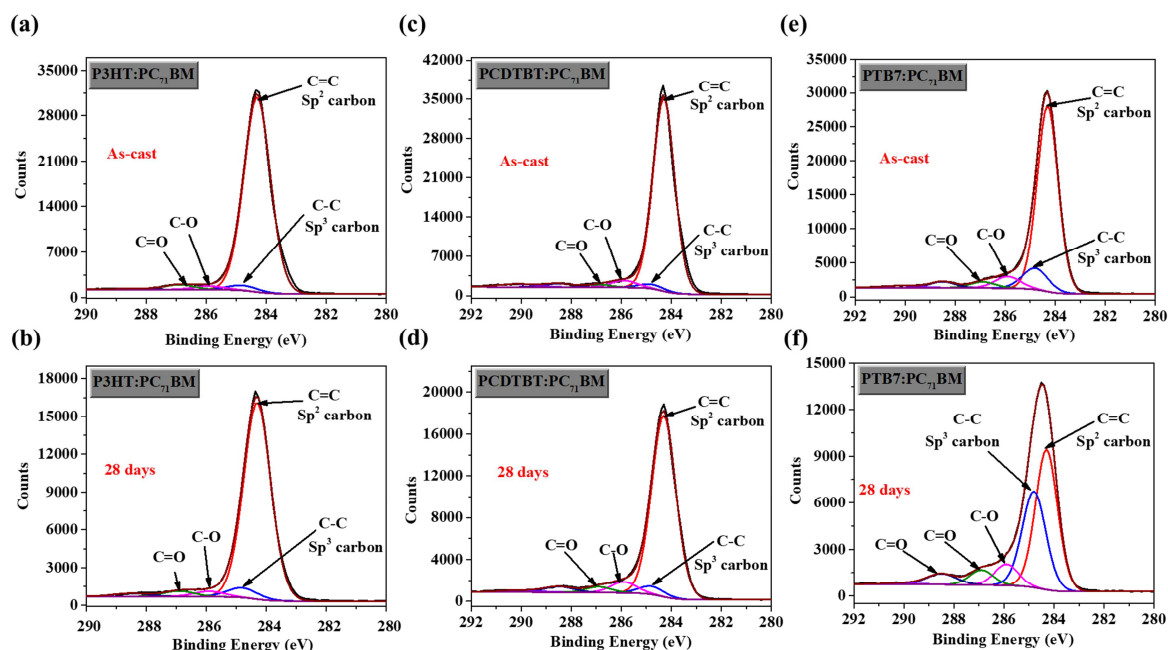
Figure 5: High resolution C1s XPS spectra of **(a, b)** P3HT:PC$_{71}$BM, **(c, d)** PCDTBT:PC$_{71}$BM and **(e, f)** PTB7:PC$_{71}$BM BHJ layers for (**above**) as cast and (**below**) after 28 days of storage in ambient air.

XPS spectra for O1s before and after the ageing in ambient air show the two components for all three BHJ samples at 531.3±0.4 eV (531.6±0.2 eV for aged samples) and 532.7±0.4 eV (533±0.4 eV for aged samples), corresponding to the C-O-C [38] (oxygen atom bonded with carbon atoms, *e.g.* ketone) and C=O bonds, that represents the oxygen atoms directly bonded with carbon atoms in the polymer backbone [39, 40]. The exact peak positions for these bonds before and after the ageing are tabulated in the **Table 3**. In addition, the PTB7:PC$_{71}$BM also shows an additional feature at 534 eV (534.3 eV for aged sample), ascribed to *O-C=O bond [41, 42]. It is noteworthy that the O1s peaks have shifted towards the higher binding energies (∼0.3eV), however, the peak position for C-O-C bond of PCDTBT:PC$_{71}$BM film did not

change. This shift in the O1s spectra indicates the oxidized states in the BHJ films [35] and attributed to the molecular interaction between the donor and acceptor segments of the BHJ system due to the morphology reconstruction [27]. These oxidized species and chemical shift after the ageing are directly coupled with the morphological instability [43].
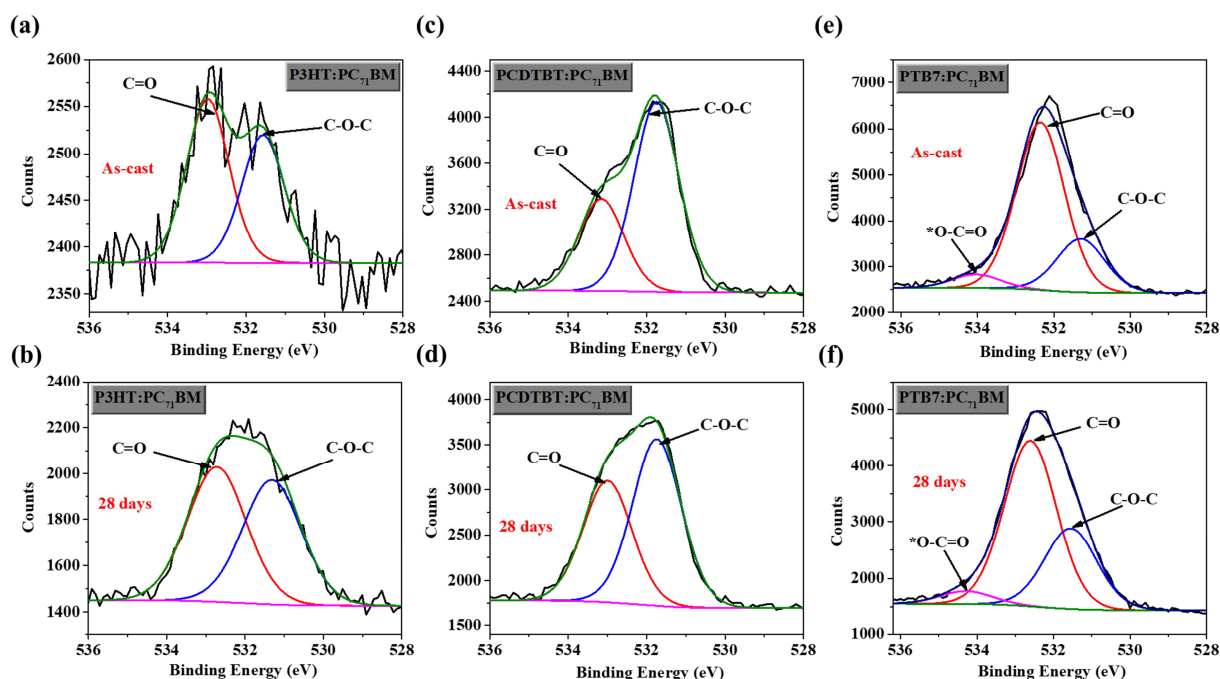

Figure 6: High resolution O1s XPS spectra of **(a, b)** P3HT:PC$_{71}$BM, **(c, d)** PCDTBT:PC$_{71}$BM and **(e, f)** PTB7:PC$_{71}$BM BHJ layers for (**above**) as cast and (**below**) after 28 days of storage in ambient air.

Table 3: XPS peak positions and corresponding chemical states of C1s and O1s high resolution spectra before and after degradation (28 days of storage in ambient air).

BHJ system		Binding energy C1s / eV				Binding energy O1s / eV		
		C=C	C-C	C-O	C=O	C-O-C	C=O	*O-C=O
P3HT:PC$_{71}$BM	As-cast					531.3	532.7	-
	Aged					531.6	533	-
PCDTBT:PC$_{71}$BM	As-cast	284.3	284.8	285.9	286.9	531.7	533	-
	Aged					531.7	533.2	-
PTB7:PC$_{71}$BM	As-cast					531.3	532.3	534
	Aged					531.6	532.6	534.3

4. DISCUSSION

The three investigated donor polymers namely; P3HT, PCDTBT and PTB7 along with the PC$_{71}$BM acceptor are the most widely utilized BHJ blends. The purpose of this study was to carry out a comparative analysis of these three BHJ layers on merits of their ambient stability and the degradation mechanisms that affect the performance of the corresponding devices. The photovoltaic results (**Table 1 and Figure 2**) indicate that the reduced J_{sc} and FF of the P3HT:PC$_{71}$BM and PTB7:PC$_{71}$BM based devices are critical factors for PCE reduction after the ageing. However, the PCDTB:PC$_{71}$BM based device showed stable J_{sc}, but similar to others, the FF has reduced to half. Also, the V_{oc} of PCDTBT:PC$_{71}$BM based device had significantly (22.62%) reduced. The J_{sc} and FF of the devices employing the corresponding materials are probably reduced due to increased charge recombination rates in the BHJ layers [27]. Particularly, in the case of PTB7:PC$_{71}$BM, sharp decrease in the J_{sc} values can be attributed to the oxygen induced degradation of the BHJ material. It is clear from the XPS data pertaining to the PTB7:PC$_{71}$BM films that photo-oxidative degradation has changed the chemical structure of the polymer. A notable reduction in carbon species (sp^2 and sp^3 carbons, peaks intensity has significantly reduced) suggests the loss of alkoxy side chains. At the same time, the oxygen bonded species have been significantly increased that indicates the formation of COOH and OH

group formation and probably the oxidation of 'S' too [19]. Oxidative species in the BHJ layer may generally function as the charge-carrier trapping sites [44, 45]. It is noteworthy that oxidative degradation may causes a sharp increase in the series resistance, which is very much a contributing factor to the reduction in the FF [27].

From the XPS data, particularly the chemical states, as well as the morphological and the optical absorbance results, the fact that P3HT:PC$_{71}$BM and PCDTB:PC$_{71}$BM based films do not possess very high degree of oxidation, and overall degradation of BHJ material is less than the corresponding decay in the photovoltaic performance, suggest that the dominating factor in the context of the device performance is probably due to interface phenomenon or oxidation of aluminum (Al) cathode. These are known vulnerable sites, because a small degree of degradation can significantly influence the electrical properties. In our recent study [29] and a study by K. Norrman *et al.* [46] it is being shown that water ingress through Al electrode forms Al oxide/hydroxide, which is an insulator. Also, the S-shaped *J-V* curves of PCDTBT:PC$_{71}$BM indicate that the interfacial degradation probably has dominated the overall efficiency loss [10, 47, 48].

In addition to the above-mentioned factors, from the perspective of the difference of the chemical structures of the three donor polymers, it is noteworthy that PTB7 is known to degrade rapidly in blends with PCBM [49]. The complex backbone structure of PTB7 is based on the combination of two units: namely, thienothiophene and benzodithiophene. The benzodithiophene unit is fringed by the two alkoxy side chains and the benzodithiophene side chain is linked to the backbone by an ester group, as shown in **Figure 1b** [50]. Also, PTB7 contains several heteroatoms that can easily get converted into free radicals upon excitation. In addition, it is noteworthy that thiophens and its derivative are inherently less stable [51]. Also, the

benzodithiophene unit is more prone to oxidation than the equivalent structures present in P3HT or PBDTBT (**Figure 1b**). The side chains on the polymer species are thought to be critical due to the potential for formation of free radicals on these side chains. The presence of oxygen helps to propagate the free radicals through the film due to its ready diffusion. In the case of PCDTBT, a free radical form on the carbon on the side chain adjacent to the carbazole group. In addition, PCDTBT also contains heteroatoms, however, there might be formation of stable radicals on its exposure.

However, regardless of the active layer, interfaces or the electrodes, the device performance or films deterioration is most likely due to oxidative degradation. Particularly, in the case of PTB7:$PC_{71}BM$ based device, the overall oxygen content has substantially increased even in the photoactive layer. In spite of the high efficiency of this material, the PTB7:$PC_{71}BM$ based devices are unstable when exposed to ambient air [52]. This is confirmed by our results as well as reported by S. Alem *et al*. [53] and Y. W. Soon *et al*. [54], the principle degradation mechanism of PTB7:$PC_{71}BM$ blend is, therefore, via photooxidation with the highly reactive oxygen species. But, as mentioned in several report, the overall degradation is very complex phenomenon, involving multiple factors such as ease of formation of stable radicals, diffusion of moisture, diffusion of oxygen and impurities. In addition, interfacial degradation, electrode and interlayer diffusion, morphological deterioration, and macroscopic changes including delamination and cracks etc. also account for majority of the performance loss [10, 55, 56].

4.1 Recent Developments in the Mechanistic Study of the Oxygen Induced Degradation of OSCs

Oxidative degradation can hinder the device stability in several ways, and it can penetrate into the device through the multiple pathways, such as; **(i)** The low work-function metal (Al) cathode gets oxidized by the oxygen penetration and consequently creates an insulating metal oxide layer between the electrode and the photoactive layer. This will eventually induce an S-shaped *J-V* curve leading to the performance degradation of the device [48, 57]. This is also evident in our results, particularly, in the case of PCDTBT:PC$_{71}$BM based devices. In addition, oxygen can penetrate through the voids and pinholes to the underneath layers in the case of longer exposure to moisture [58, 59]. This has also been demonstrated and discussed in our previous works [29, 56]. **(ii)** The oxidative atmosphere in the BHJ layer contributes towards the several photo-oxidation reactions of donor-acceptor segments of the BHJ material [60, 61]. Ultimately, the energy levels as well as the charge carriers mobilities get disruptive owing to the oxygen penetration. **(iii)** The oxygen doping in the BHJ layer can potentially increase the hole concentration, resulting in an enhanced density of deeper traps for electrons. As a result, it leads to the reduction in the FF and V$_{oc}$, as evident in our results too (**Table 2**) [62, 63]. **(iv)** Likewise, oxygen is accountable for the majority of the loss in the J$_{sc}$ due to exciton quenching. In addition, V$_{oc}$ reduces due to enhanced saturation current in conjunction with the reduction in the generation of charge-carriers owing to the exciton quenching [64]. **Figure 7** illustrates some of the oxygen and water induced degradation pathways.
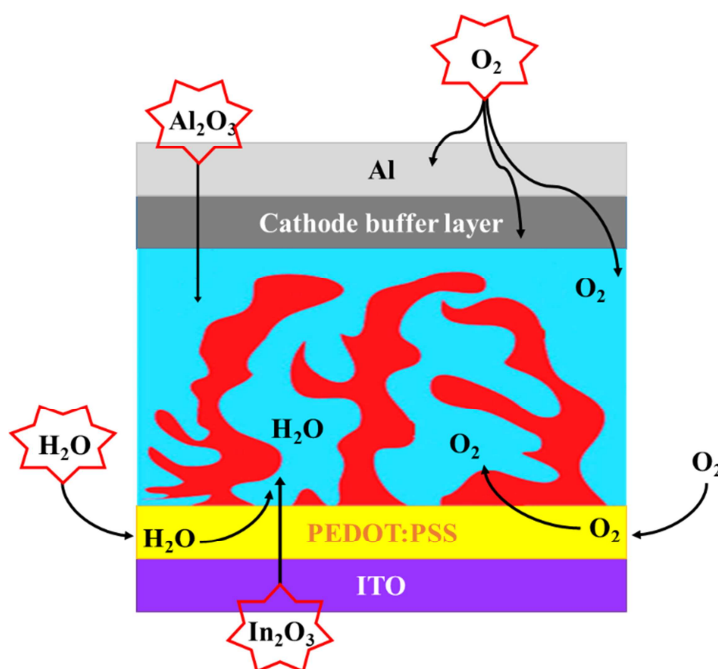
Figure 7: Schematic diagram of oxidative and water induced degradation pathways

In addition to the above-mentioned degradation factors, the chemical structure of the polymers is also critical in terms of degradation. For example, the PTB7 both in neat films and in blends with $PC_{71}BM$ possesses photooxidative degradation with the highly reactive singlet O_2 species generated from triplet excitons [53, 54]. The singlet oxygen is produced in PTB7 blends owing to PTB7 triplet generated by non-geminate charge recombination. According to Soon *et al.* [54], the triplet state of PTB7 possess sufficient energy to generate singlet oxygen. Same is the case when it is blended with $PC_{71}BM$. PTB7 when blended with $PC_{71}BM$ leads to accelerated polymer's degradation due to the increased production of singlet oxygen [49], which strongly indicates that (as indicated in our results too) the faster degradation in the presence of oxygen derives from triplet mediated singlet oxygen generation. Hence, degradation in the $PTB7:PC_{71}BM$ blend can be ascribed to the oxygen quenching of triplets induced by the non-geminate recombination of dissociated polarons [54], and not the anionic radical O_2^- superoxide

generation by charge transfer from the polymer, as described by Razzell-Hollis *et.al.* [49]. The performance loss is also ascribed to photobleaching and absorbance loss during the degradation, as evident in our results too. However, the P3HT:PC$_{71}$BM experienced pronounced decrease in the J$_{sc}$ and FF which is mainly influenced by the processes related to the exciton generation and diffusion in P3HT domain [65]. The photo-oxidation causes the chemical degradation of P3HT in terms of crystallinity loss which consequently forms the gap-states. Although, these degradation processes do not notably alter absorption spectra or morphology, however PCE can be significantly decreased, mainly, owing to the increase of the exciton recombination in P3HT domains resulting in the photocurrent decrease, as evident in our results too [65].

It is thus concluded that oxygen is the main cause of device degradation in all three BHJ donor-acceptor materials with PCDTBT:PC$_{71}$BM BHJ material being the most stable among all three bench-marked materials and PTB7:PC$_{71}$BM in spite of the highest efficiency was observed to be the least stable. FF was determined to be the critical factor in PCE loss among these materials along with the significant loss in the J$_{sc}$ (not in the case of PCDTBT:PC$_{71}$BM based devices).

5. CONCLUSIONS

We investigated and compared the effect of ambient atmosphere on stability/degradation of P3HT:PC$_{71}$BM, PCDTBT:PC$_{71}$BM and PTB7:PC$_{71}$BM BHJ layers in both films and devices. The loss of PCE of the devices exposed to ambient air is largely due to the drastic decrease in the FF of the three BHJ systems followed by a pronounced decrease in the J$_{sc}$ of P3HT:PC$_{71}$BM (33.87%) and PTB7:PC$_{71}$BM (45.87%) based devices. However, the PCDTBT based device showed only 7.13% J$_{sc}$ loss over 14 days. The V$_{oc}$ observed to be remained relatively stable for

all three variants. Overall, the device comprising PCDTBT:PC$_{71}$BM BHJ layer showed the highest stability and PTB7:PC$_{71}$BM based devices observed to be the least stable. XPS data confirms the oxidation of polymers:fullerene blend after ageing and appeared to be typical of oxygen-containing materials. Particularly, the PTB7:PC$_{71}$BM showed substantial increase in the oxygen content that reached up to 10.5% in 28 days. Also, the oxygen-containing bonds (e.g. C-O and C=O bonds) have become prominent after the degradation. The peak shift in the O1s spectra indicates the change in the molecular interaction between the donor and acceptor segments owing to the morphology reconstruction. AFM and UV-visible results also confirm the increased surface roughness and decay in the absorbance of PTB7:PC$_{71}$BM films after ageing. However, both the P3HT:PC$_{71}$BM and PCDTBT:PC$_{71}$BM samples demonstrated relatively stable morphology and insignificant loss in the absorbance. In conclusion, the current study provides a detailed comparative analysis of the three most commonly employed BHJ donor-acceptor materials. It can help in material selection and addressing the stability challenges by considering the stability/degradation factors discussed in this work. Although, a lot more work is needed to be done, however, the promise of OSCs as being the future solar energy source is greater than ever.

ACKNOWLEDGMENTS

REFERENCES

[1] C.J. Brabec, N.S. Sariciftci, J.C. Hummelen, Plastic solar cells, Advanced functional materials, 11 (2001) 15-26.

[2] T. Ameri, G. Dennler, C. Lungenschmied, C.J. Brabec, Organic tandem solar cells: A review, Energy & Environmental Science, 2 (2009) 347-363.

[3] B.C. Thompson, J.M. Fréchet, Polymer–fullerene composite solar cells, Angewandte chemie international edition, 47 (2008) 58-77.

[4] C. Sun, F. Pan, H. Bin, J. Zhang, L. Xue, B. Qiu, Z. Wei, Z.-G. Zhang, Y. Li, A low cost and high performance polymer donor material for polymer solar cells, Nature communications, 9 (2018) 743.

[5] C. Liu, C. Yi, K. Wang, Y. Yang, R.S. Bhatta, M. Tsige, S. Xiao, X. Gong, Single-junction polymer solar cells with over 10% efficiency by a novel two-dimensional donor–acceptor conjugated copolymer, ACS applied materials & interfaces, 7 (2015) 4928-4935.

[6] S. Rohr, Heliatek consolidates its technology leadership by establishing a new world record for organic solar technology with a cell efficiency of 12%, Press release Heliatek GmbH, (2013).

[7] J. Zhao, Y. Li, G. Yang, K. Jiang, H. Lin, H. Ade, W. Ma, H. Yan, Efficient organic solar cells processed from hydrocarbon solvents, Nature Energy, 1 (2016) 15027.

[8] S. Zhang, L. Ye, J. Hou, Breaking the 10% Efficiency Barrier in Organic Photovoltaics: Morphology and Device Optimization of Well□Known PBDTTT Polymers, Advanced Energy Materials, 6 (2016) 1502529.

[9] J. Hou, O. Inganäs, R.H. Friend, F. Gao, Organic solar cells based on non-fullerene acceptors, Nature materials, 17 (2018) 119.

[10] K. Norrman, M.V. Madsen, S.A. Gevorgyan, F.C. Krebs, Degradation patterns in water and oxygen of an inverted polymer solar cell, Journal of the American Chemical Society, 132 (2010) 16883-16892.

[11] D. Chi, S. Qu, Z. Wang, J. Wang, High efficiency P3HT: PCBM solar cells with an inserted PCBM layer, Journal of Materials Chemistry C, 2 (2014) 4383-4387.

[12] S. Holliday, R.S. Ashraf, A. Wadsworth, D. Baran, S.A. Yousaf, C.B. Nielsen, C.-H. Tan, S.D. Dimitrov, Z. Shang, N. Gasparini, High-efficiency and air-stable P3HT-based polymer solar cells with a new non-fullerene acceptor, Nature communications, 7 (2016) 11585.

[13] S. Rafique, S.M. Abdullah, M.M. Shahid, M.O. Ansari, K. Sulaiman, Significantly improved photovoltaic performance in polymer bulk heterojunction solar cells with graphene oxide/PEDOT: PSS double decked hole transport layer, Scientific reports, 7 (2017) 39555.

[14] F. Etzold, I.A. Howard, R. Mauer, M. Meister, T.-D. Kim, K.-S. Lee, N.S. Baek, F. Laquai, Ultrafast exciton dissociation followed by nongeminate charge recombination in PCDTBT: PCBM photovoltaic blends, Journal of the American Chemical Society, 133 (2011) 9469-9479.

[15] N. Banerji, S. Cowan, M. Leclerc, E. Vauthey, A.J. Heeger, Exciton formation, relaxation, and decay in PCDTBT, Journal of the American Chemical Society, 132 (2010) 17459-17470.

[16] B. Ebenhoch, S.A. Thomson, K. Genevičius, G. Juška, I.D. Samuel, Charge carrier mobility of the organic photovoltaic materials PTB7 and PC71BM and its influence on device performance, Organic Electronics, 22 (2015) 62-68.

[17] I. Etxebarria, A. Guerrero, J. Albero, G. Garcia-Belmonte, E. Palomares, R. Pacios, Inverted vs standard PTB7: PC70BM organic photovoltaic devices. The benefit of highly selective and extracting contacts in device performance, Organic Electronics, 15 (2014) 2756-2762.

[18] Z. Ding, J. Kettle, M. Horie, S.-W. Chang, G.C. Smith, A.I. Shames, E.A. Katz, Efficient solar cells are more stable: the impact of polymer molecular weight on performance of organic photovoltaics, Journal of Materials Chemistry A, 4 (2016) 7274-7280.

[19] J. Kettle, Z. Ding, M. Horie, G. Smith, XPS analysis of the chemical degradation of PTB7 polymers for organic photovoltaics, Organic Electronics, 39 (2016) 222-228.

[20] J. Chang, Z. Lin, C. Jiang, J. Zhang, C. Zhu, J. Wu, Improve the operational stability of the inverted organic solar cells using bilayer metal oxide structure, ACS applied materials & interfaces, 6 (2014) 18861-18867.

[21] Z. Shi, H. Liu, Y. Wang, J. Li, Y. Bai, F. Wang, X. Bian, T. Hayat, A. Alsaedi, Z.a. Tan, Incorporating an electrode modification layer with a vertical phase separated photoactive layer for efficient and stable inverted nonfullerene polymer solar cells, ACS applied materials & interfaces, 9 (2017) 43871-43879.

[22] C. Sprau, F. Buss, M. Wagner, D. Landerer, M. Koppitz, A. Schulz, D. Bahro, W. Schabel, P. Scharfer, A. Colsmann, Highly efficient polymer solar cells cast from non-halogenated xylene/anisaldehyde solution, Energy & Environmental Science, 8 (2015) 2744-2752.

[23] B.A. Collins, Z. Li, J.R. Tumbleston, E. Gann, C.R. McNeill, H. Ade, Absolute measurement of domain composition and nanoscale size distribution explains performance in PTB7: PC71BM solar cells, Advanced Energy Materials, 3 (2013) 65-74.

[24] Y. Liang, Z. Xu, J. Xia, S.T. Tsai, Y. Wu, G. Li, C. Ray, L. Yu, For the bright future—bulk heterojunction polymer solar cells with power conversion efficiency of 7.4%, Advanced materials, 22 (2010) E135-E138.

[25] F. Liu, W. Zhao, J.R. Tumbleston, C. Wang, Y. Gu, D. Wang, A.L. Briseno, H. Ade, T.P. Russell, Understanding the morphology of PTB7: PCBM blends in organic photovoltaics, Advanced Energy Materials, 4 (2014) 1301377.

[26] J. Kettle, H. Waters, Z. Ding, M. Horie, G.C. Smith, Chemical changes in PCPDTBT: PCBM solar cells using XPS and TOF-SIMS and use of inverted device structure for improving lifetime performance, Solar Energy Materials and Solar Cells, 141 (2015) 139-147.

[27] D.H. Wang, J.K. Kim, J.H. Seo, O.O. Park, J.H. Park, Stability comparison: A PCDTBT/PC71BM bulk-heterojunction versus a P3HT/PC71BM bulk-heterojunction, Solar Energy Materials and Solar Cells, 101 (2012) 249-255.

[28] S. Cho, J.H. Seo, S.H. Park, S. Beaupré, M. Leclerc, A.J. Heeger, A thermally stable semiconducting polymer, Advanced Materials, 22 (2010) 1253-1257.

[29] S. Rafique, S.M. Abdullah, K. Sulaiman, M. Iwamoto, Layer by layer characterisation of the degradation process in PCDTBT: PC71BM based normal architecture polymer solar cells, Organic Electronics, 40 (2017) 65-74.

[30] G. Beamson, High resolution XPS of organic polymers, The Scienta ESCA 300 Database, (1992).

[31] D. Wang, Y. Hu, J. Zhao, L. Zeng, X. Tao, W. Chen, Holey reduced graphene oxide nanosheets for high performance room temperature gas sensing, Journal of Materials Chemistry A, 2 (2014) 17415-17420.

[32] X.-C. Li, F.-S. She, D. Shen, C.-P. Liu, L.-H. Chen, Y. Li, Z. Deng, Z.-H. Chen, H.-E. Wang, Coherent nanoscale cobalt/cobalt oxide heterostructures embedded in porous carbon for the oxygen reduction reaction, RSC Advances, 8 (2018) 28625-28631.

[33] C. Mattevi, G. Eda, S. Agnoli, S. Miller, K.A. Mkhoyan, O. Celik, D. Mastrogiovanni, G. Granozzi, E. Garfunkel, M. Chhowalla, Evolution of electrical, chemical, and structural properties of transparent and conducting chemically derived graphene thin films, Advanced Functional Materials, 19 (2009) 2577-2583.

[34] H.-W. Tien, Y.-L. Huang, S.-Y. Yang, J.-Y. Wang, C.-C.M. Ma, The production of graphene nanosheets decorated with silver nanoparticles for use in transparent, conductive films, Carbon, 49 (2011) 1550-1560.

[35] J. Jeong, J. Seo, S. Nam, H. Han, H. Kim, T.D. Anthopoulos, D.D. Bradley, Y. Kim, Significant Stability Enhancement in High□Efficiency Polymer: Fullerene Bulk Heterojunction Solar Cells by Blocking Ultraviolet Photons from Solar Light, Advanced Science, 3 (2016) 1500269.

[36] E.M. Speller, A.J. Clarke, N. Aristidou, M.F. Wyatt, L. Francàs, G. Fish, H. Cha, H.K.H. Lee, J. Luke, A. Wadsworth, Toward Improved Environmental Stability of Polymer: Fullerene and Polymer: Nonfullerene Organic Solar Cells: A Common Energetic Origin of Light-and Oxygen-Induced Degradation, ACS Energy Letters, 4 (2019) 846-852.

[37] M. Hermenau, M. Riede, K. Leo, S.A. Gevorgyan, F.C. Krebs, K. Norrman, Water and oxygen induced degradation of small molecule organic solar cells, Solar Energy Materials and Solar Cells, 95 (2011) 1268-1277.

[38] A.R. bin Mohd Yusoff, H.P. Kim, J. Jang, High performance organic photovoltaics with zinc oxide and graphene oxide buffer layers, Nanoscale, 6 (2014) 1537-1544.

[39] K.L. Mittal, Polymer surface modification: relevance to adhesion, CRC Press, 2004.

[40] B. Schweiger, J. Kim, Y. Kim, M. Ulbricht, Electropolymerized molecularly imprinted polypyrrole film for sensing of clofibric acid, Sensors, 15 (2015) 4870-4889.

[41] J. Yang, X. Yan, J. Chen, H. Ma, D. Sun, Q. Xue, Comparison between metal ion and polyelectrolyte functionalization for electrophoretic deposition of graphene nanosheet films, RSC Advances, 2 (2012) 9665-9670.

[42] S.K. Das, C. Dickinson, F. Lafir, D.F. Brougham, E. Marsili, Synthesis, characterization and catalytic activity of gold nanoparticles biosynthesized with Rhizopus oryzae protein extract, Green Chemistry, 14 (2012) 1322-1334.

[43] G. Li, V. Shrotriya, J. Huang, Y. Yao, T. Moriarty, K. Emery, Y. Yang, High-efficiency solution processable polymer photovoltaic cells by self-organization of polymer blends, in: Materials For Sustainable Energy: A Collection of Peer-Reviewed Research and Review Articles from Nature Publishing Group, World Scientific, 2011, pp. 80-84.

[44] B. Paci, A. Generosi, V.R. Albertini, P. Perfetti, R. De Bettignies, C. Sentein, Photo-degradation and stabilization effects in operating organic photovoltaic devices by joint photo-current and morphological monitoring, Solar Energy Materials and Solar Cells, 92 (2008) 799-804.

[45] A. Kumar, Z. Hong, S. Sista, Y. Yang, The critical role of processing and morphology in determining degradation rates in polymer solar cells, Advanced Energy Materials, 1 (2011) 124-131.

[46] K. Norrman, S.A. Gevorgyan, F.C. Krebs, Water-induced degradation of polymer solar cells studied by H218O labeling, ACS applied materials & interfaces, 1 (2008) 102-112.

[47] M.R. Lilliedal, A.J. Medford, M.V. Madsen, K. Norrman, F.C. Krebs, The effect of post-processing treatments on inflection points in current–voltage curves of roll-to-roll processed polymer photovoltaics, Solar Energy Materials and Solar Cells, 94 (2010) 2018-2031.

[48] M. Glatthaar, M. Riede, N. Keegan, K. Sylvester-Hvid, B. Zimmermann, M. Niggemann, A. Hinsch, A. Gombert, Efficiency limiting factors of organic bulk heterojunction solar cells identified by electrical impedance spectroscopy, Solar Energy Materials and Solar Cells, 91 (2007) 390-393.

[49] J. Razzell-Hollis, J. Wade, W.C. Tsoi, Y. Soon, J. Durrant, J.-S. Kim, Photochemical stability of high efficiency PTB7: PC 70 BM solar cell blends, Journal of Materials Chemistry A, 2 (2014) 20189-20195.

[50] A. Perthué, T. Gorisse, H.S. Silva, D. Bégué, A. Rivaton, G. Wantz, Influence of traces of oxidized polymer on the performances of bulk heterojunction solar cells, Materials Chemistry Frontiers, (2019).

[51] N.Y. Doumon, G. Wang, R.C. Chiechi, L.J.A. Koster, Relating polymer chemical structure to the stability of polymer: fullerene solar cells, Journal of Materials Chemistry C, 5 (2017) 6611-6619.

[52] D. Bartesaghi, G. Ye, R.C. Chiechi, L.J.A. Koster, Compatibility of PTB7 and [70] PCBM as a Key Factor for the Stability of PTB7:[70] PCBM Solar Cells, Advanced Energy Materials, 6 (2016) 1502338.

[53] S. Alem, S. Wakim, J. Lu, G. Robertson, J. Ding, Y. Tao, Degradation mechanism of benzodithiophene-based conjugated polymers when exposed to light in air, ACS applied materials & Interfaces, 4 (2012) 2993-2998.

[54] Y.W. Soon, H. Cho, J. Low, H. Bronstein, I. McCulloch, J.R. Durrant, Correlating triplet yield, singlet oxygen generation and photochemical stability in polymer/fullerene blend films, Chemical Communications, 49 (2013) 1291-1293.

[55] V. Sharma, V. Singh, M. Arora, S. Arora, R. Tandon, Degradation analysis of PCDTBT: PC71BM organic solar cells-an insight, Current Applied Physics, 16 (2016) 273-277.

[56] S. Rafique, S.M. Abdullah, K. Sulaiman, M. Iwamoto, Fundamentals of bulk heterojunction organic solar cells: An overview of stability/degradation issues and strategies for improvement, Renewable and Sustainable Energy Reviews, 84 (2018) 43-53.

[57] B.Y. Finck, B.J. Schwartz, Understanding the origin of the S-curve in conjugated polymer/fullerene photovoltaics from drift-diffusion simulations, Applied Physics Letters, 103 (2013) 143_141.

[58] K. Kawano, R. Pacios, D. Poplavskyy, J. Nelson, D.D. Bradley, J.R. Durrant, Degradation of organic solar cells due to air exposure, Solar energy materials and solar cells, 90 (2006) 3520-3530.

[59] M. Seeland, R. Rösch, H. Hoppe, Luminescence imaging of polymer solar cells: Visualization of progressing degradation, Journal of Applied Physics, 109 (2011) 064513.

[60] K. Norrman, F.C. Krebs, Lifetimes of organic photovoltaics: using TOF-SIMS and 18O2 isotopic labelling to characterise chemical degradation mechanisms, Solar Energy Materials and Solar Cells, 90 (2006) 213-227.

[61] M.O. Reese, A.M. Nardes, B.L. Rupert, R.E. Larsen, D.C. Olson, M.T. Lloyd, S.E. Shaheen, D.S. Ginley, G. Rumbles, N. Kopidakis, Photoinduced degradation of polymer and polymer–fullerene active layers: experiment and theory, Advanced Functional Materials, 20 (2010) 3476-3483.

[62] J. Schafferhans, A. Baumann, A. Wagenpfahl, C. Deibel, V. Dyakonov, Oxygen doping of P3HT: PCBM blends: Influence on trap states, charge carrier mobility and solar cell performance, Organic Electronics, 11 (2010) 1693-1700.

[63] A. Seemann, T. Sauermann, C. Lungenschmied, O. Armbruster, S. Bauer, H.-J. Egelhaaf, J. Hauch, Reversible and irreversible degradation of organic solar cell performance by oxygen, Solar Energy, 85 (2011) 1238-1249.

[64] J.o.P. Bastos, E. Voroshazi, E. Fron, G. Brammertz, T. Vangerven, M. Van der Auweraer, J. Poortmans, D. Cheyns, Oxygen-induced degradation in C60-based organic solar cells: Relation between film properties and device performance, ACS applied materials & interfaces, 8 (2016) 9798-9805.

[65] J. Müllerová, M. Kaiser, V. Nádaždy, P. Šiffalovič, E. Majková, Optical absorption study of P3HT: PCBM blend photo-oxidation for bulk heterojunction solar cells, Solar Energy, 134 (2016) 294-301.

Highlights:

- Stability/degradation analysis of organic solar cells has been reported.

- Comparative study of benchmarked donor polymers is presented.

- Degradation issues of the absorption layer have been investigated.

- Oxygen induced performance loss in ambient air is identified.

- Optical, chemical, morphological, compositional and electrical study have been conducted.